



Scholars Research Library

Der Pharma Chemica, 2014, 6(2):239-251  
(<http://derpharmachemica.com/archive.html>)



ISSN 0975-413X  
CODEN (USA): PCHHAX

## Exploring structural stability and electronic properties of SnSe nanostructures-A DFT study

V. Nagarajan and R. Chandiramouli\*

School of Electrical & Electronics Engineering, SASTRA University, Tirumalaisamudram, Thanjavur, India

### ABSTRACT

The realistic nanostructure of pure, defect structure, cadmium and sulfur substituted cube & hexagonal SnSe nanostructures are optimized and successfully simulated using B3LYP/LanL2DZ basis set. The structural stability of SnSe nanostructures are discussed in terms of calculated energy and vibrational studies. The ionization potential, electron affinity and HOMO – LUMO gap influence the electronic properties of SnSe nanostructures. The point group, dipole moment, chemical hardness and chemical potential for pure, defect structure and cadmium & sulfur substituted SnSe nanostructures are also reported. The present work provides the information to tailor SnSe nanostructures by substitution impurities and defect in the nanostructure that improves the electronic properties and structural stability which finds its potential importance in optoelectronic applications.

**Keywords:** tin selenide, chemical hardness, chemical potential, vibrational studies, HOMO, LUMO

### INTRODUCTION

Nanostructured materials play a vital role in future technology mainly in optoelectronics, nanoelectronics and memory devices [1]. In present years more attention are focused on to the synthesis and characteristics of selenides due to their potential application and tunable properties. Tin selenide (SnSe) is one of the most important group IV – VI compound semiconductor. SnSe is a p – type semiconductor with narrow band gap energy of 1 eV which is applicable for different optoelectronics application such as photovoltaic, memory switching devices, holographic recording systems and light emitting devices (LEDs) [2-4].

SnSe nanostructures have good electrical and optical properties which mainly depend on preparation technique. N.R.Mathews *et al.*, reported CdS/SnSe heterojunction thin films for photovoltaic applications [3]. SnSe thin films can be synthesized by different techniques such as thermal evaporation [5, 6], chemical bath deposition [7], flash deposition [8], atomic layer deposition [9] and hot wall epitaxy [10]. Thermal evaporation method is mostly used among them due to its tunable morphology in SnSe nanostructures.

The main goal behind this work is to improve the electronic properties, structural stability of SnSe nanostructures by substitution impurities. Density functional theory (DFT) is one of the promising methods to enhance both electronic, optical properties and structural stability of SnSe nanostructures. DFT method is an efficient method to investigate electronic properties of SnSe nanostructures [11-13].

### MATERIALS AND METHODS

#### COMPUTATIONAL METHODS

NWChem package is promising simulation software used to investigate and optimize SnSe nanostructures [14]. Utilizing B3LYP with combination of LanL2DZ basis set, SnSe nanostructures are successfully optimized.

LanL2DZ basis set is the best choice to get precise throughput and pseudo potential approximation [15-20]. Since atomic number of Sn and Se is fifty and thirty four respectively, LanL2DZ basis set can be selected to study SnSe nanostructures. In this current work, various suitable dopant elements are substituted on pure SnSe nanostructures in order to tailor structural stability and electronic properties.

## RESULTS AND DISCUSSION

The present work mainly focus on calculated energy, dipole moment (DM), ionization potential (IP), electron affinity (EA), chemical potential (CP), chemical hardness (CH), HOMO – LUMO gap and vibrational studies of SnSe nanostructure with substitution of cadmium, sulfur and inclusion of defects in SnSe nanostructure. Figure 1 (a) and Figure 1(b) represents the pure form of SnSe nanostructure of cube and hexagonal structure respectively. Figure 1 (c) and Figure 1(d) denotes the cube and hexagonal structure of SnSe nanostructure with defects. Figure 1 (e) and Figure 1(f) represents cadmium substituted SnSe nanostructure. Figure 1 (g) and Figure 1(h) signifies sulfur substituted SnSe nanostructure. The pure cube SnSe nanostructure consists of six Sn atoms and six Se atoms to form cube like structure. The pure hexagonal SnSe nanostructure contains nine Sn atoms and nine Se atoms to form hexagonal structure. Defect incorporated SnSe cube structure have five Sn atoms & five Se atoms and defect SnSe hexagonal structure have eight Sn atoms & eight Se atoms respectively. In the case of cube and hexagonal structures of Cd substituted SnSe have two Cd atoms replaced instead of Sn atoms. Likewise, for cube and hexagonal structures of S substituted SnSe have two S atoms replaced for Se atoms.

Figure 1 (a). Structure of pure cube SnSe nanostructures

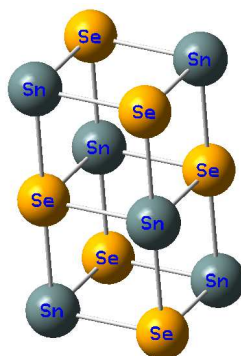


Figure 1 (b). Structure of pure hexagonal SnSe nanostructures

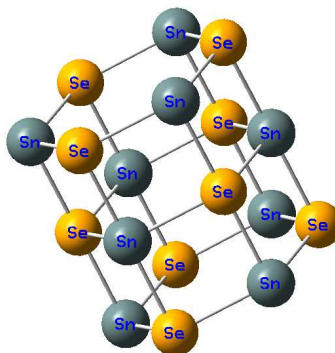


Figure 1 (c). Structure of defect cube SnSe nanostructures

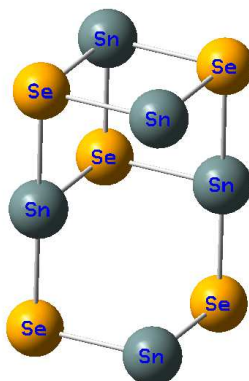


Figure 1 (d). Structure of defect hexagonal SnSe nanostructures

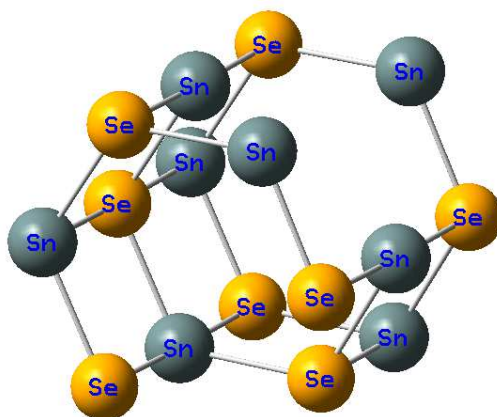


Figure 1 (e). Structure of Cd substituted cube SnSe nanostructures

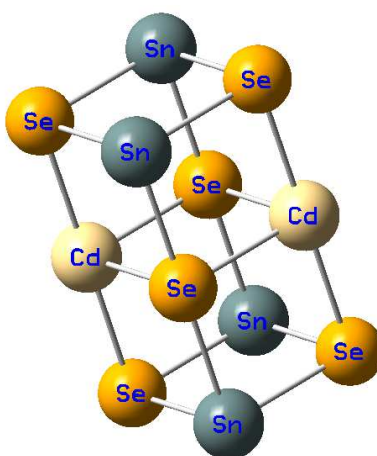


Figure 1 (f). Structure of Cd substituted hexagonal SnSe nanostructures

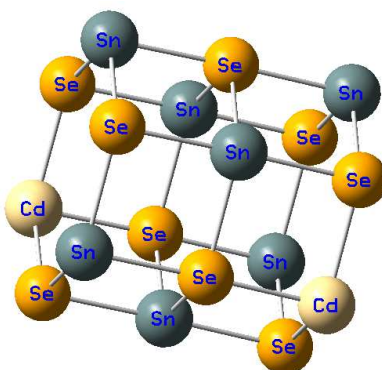


Figure 1 (g). Structure of S substituted cube SnSe nanostructures

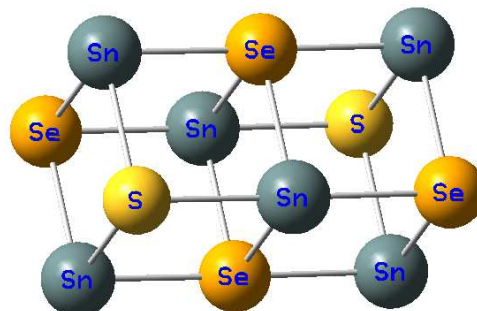


Figure 1 (h). Structure of S substituted hexagonal SnSe nanostructures

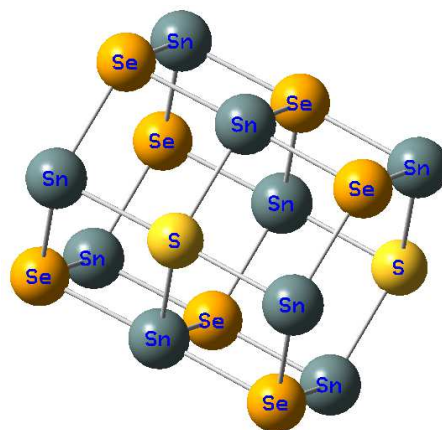


Table 1. Energy, Point symmetry and Dipole moment of SnSe nanostructures


Nanostructures	Energy (Hartrees)	Dipole moment (Debye)	Point Group
Pure cube SnSe	-74.12	0.028	C <sub>1</sub>
Pure hexagonal SnSe	-111.25	0.54	C <sub>1</sub>
defect cube SnSe	-62.21	2.81	C <sub>1</sub>
defect hexagonal SnSe	-99.34	2.14	C <sub>1</sub>
Cd substituted cube SnSe	-163.84	0.028	C <sub>1</sub>
Cd substituted hexagonal SnSe	-200.79	4.15	C <sub>1</sub>
S substituted cube SnSe	-76.06	0.032	C <sub>1</sub>
S substituted hexagonal SnSe	-133.23	0.41	C <sub>1</sub>

The SnSe nanostructures structural stability can be described by calculated energy as shown in Table 1. Point group (PG) and dipole moment (DM) of all possible SnSe nanostructures are also reported in Table 1. The calculated energy of pure cube and hexagonal SnSe nanostructure has -74.12 and -111.25 Hartrees respectively. Defect cube and hexagonal SnSe nanostructures has the corresponding calculated energy of -62.21 and -99.34 Hartrees. From the calculated energies, the stability of the defect SnSe nanostructure decreases due to the removal of atoms. Cd substituted cube and hexagonal SnSe nanostructures has the energy value of -163.84 and -200.79 Hartrees. Hence the stability of SnSe nanostructure increases due to the substitution of Cd atoms on SnSe nanostructures. Similarly for S substituted cube and hexagonal SnSe nanostructures, the calculated energy value is high compared to pure form of SnSe nanostructures; it leads to increase in the structural stability. The dipole moment of defect cube & hexagonal SnSe nanostructure, Cd substituted hexagonal SnSe nanostructure has high value of DM in the order of 2.81, 2.14 and 4.15 Debye respectively. Hence the charge distribution is not uniform in these structures. The remaining structures of SnSe nanostructure have sufficiently low value in the range 0.028 – 0.54 Debye. It reveals that the arrangement of atoms and the charge distribution are uniform inside the SnSe nanostructures. C<sub>1</sub> has only one symmetry operation, E. Nanostructures in this group have no symmetry, it refers that reflection of a mirror plane and rotation operations are not possible in SnSe nanostructures and the only symmetry operation possible in SnSe nanostructure is identity, E. All the nanostructures of SnSe have C<sub>1</sub> symmetry.

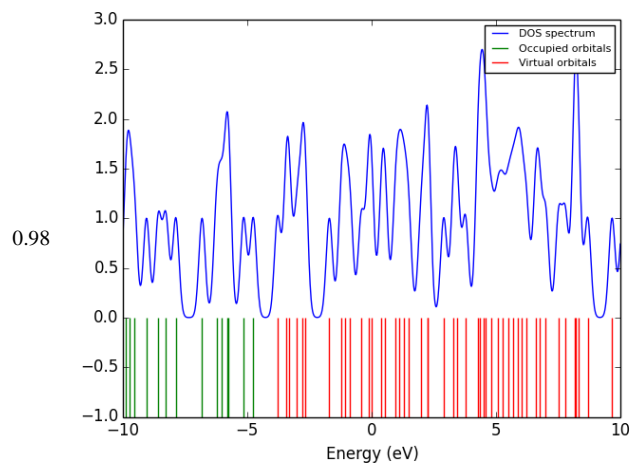
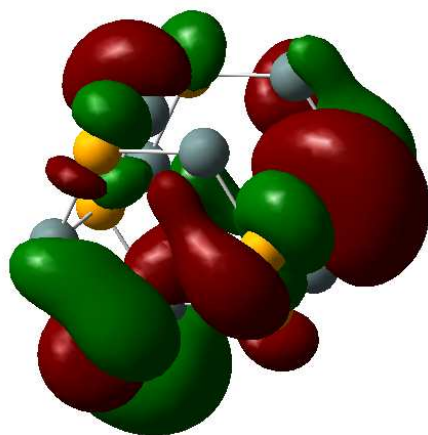
### 3.1. HOMO-LUMO gap of SnSe nanostructures

The electronic properties of SnSe nanostructures can be observed by lowest unoccupied molecular orbital (LUMO) and highest occupied molecular orbital (HOMO) [21, 22]. The energy gap of pure cube & hexagonal SnSe nanostructures has 0.66 and 0.47 eV respectively. The defect cube and hexagonal SnSe nanostructure has the energy gap of 1.41 and 0.98 eV respectively, it shows that the conductivity decreases due to removal of atoms from SnSe nanostructures. When substituting Cd on SnSe nanostructures, the resistivity increases due to increase in HOMO – LUMO gap. The energy gap of Cd substituted cube & hexagonal SnSe nanostructures is 2.01 and 0.61 eV respectively. Similarly the energy gap of S substituted hexagonal SnSe nanostructure slightly increases to a value of 0.61 eV. In contrast the energy gap of S substituted cube SnSe nanostructures decreases to 0.57 eV. Hence the conductivity increases due to substitution of sulfur on cube SnSe nanostructures but not in the case of hexagonal SnSe nanostructures. Table 2 shows the visualization of HOMO – LUMO gap and density of states (DOS). In this work, the energy gap values are observed in the range from 0.56 – 2.01 eV. It reveals that the SnSe nanostructure is a semiconductor with low energy gap value which is applicable to different optoelectronics application. The localization of charges is observed in LUMO level which is inferred from more number of peaks in virtual orbital. The substitution impurities modify the density of states in SnSe nanostructures.

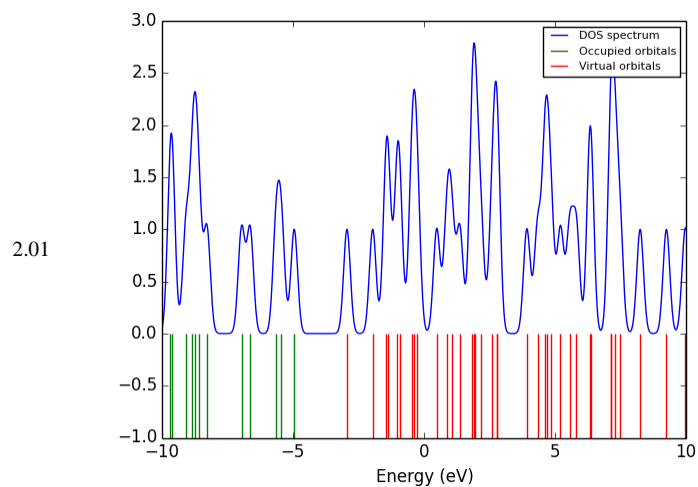
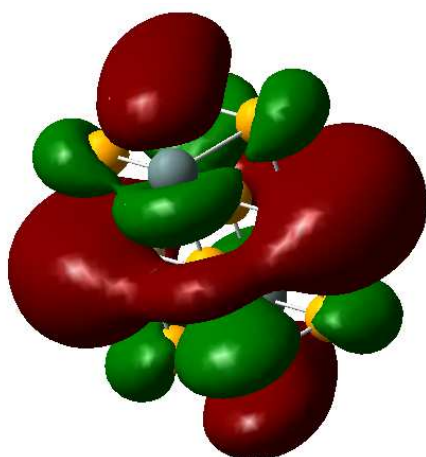
Table 2. HOMO-LUMO gap and density of states of SnSe nanostructures

Nano structures	HOMO – LUMO Visualization 	$E_g$ (eV)	HOMO, LUMO and DOS Spectrum
Pure cube SnSe		0.66	
Pure hexagonal SnSe		0.47	
defect cube SnSe		1.41	

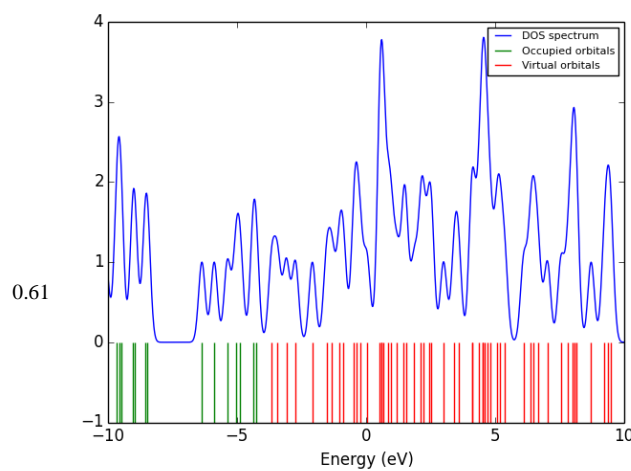
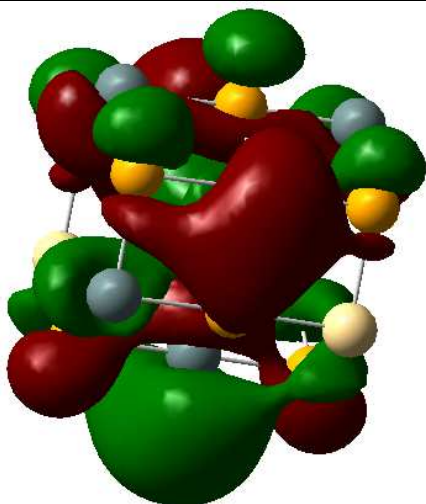
defect hexagonal SnSe



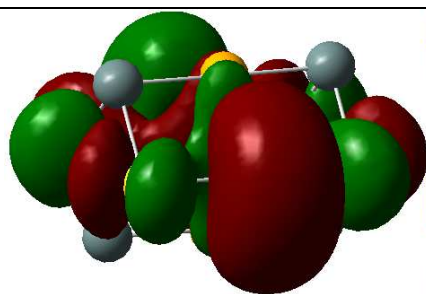
Cd substituted cube SnSe



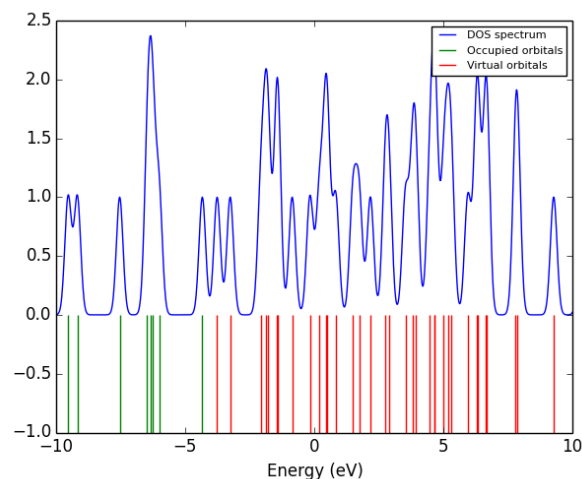
Cd substituted hexagonal SnSe



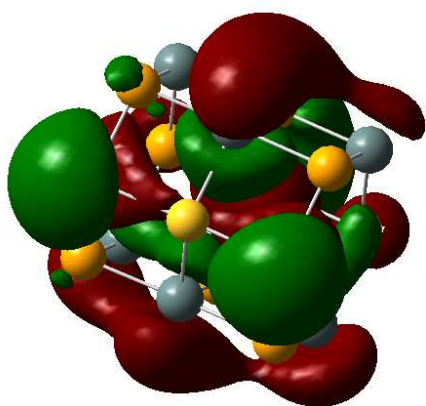
S substituted cube SnSe



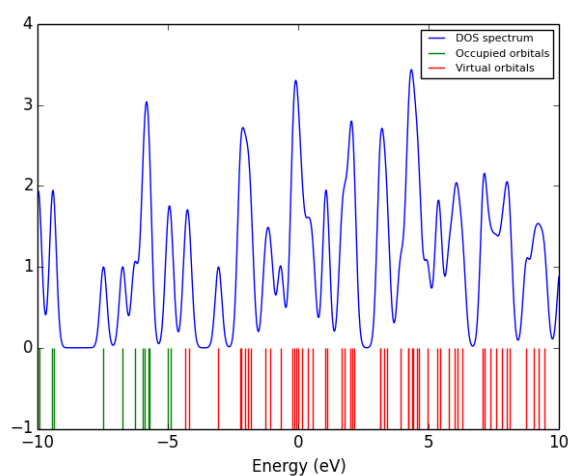
0.57



S substituted hexagonal SnSe



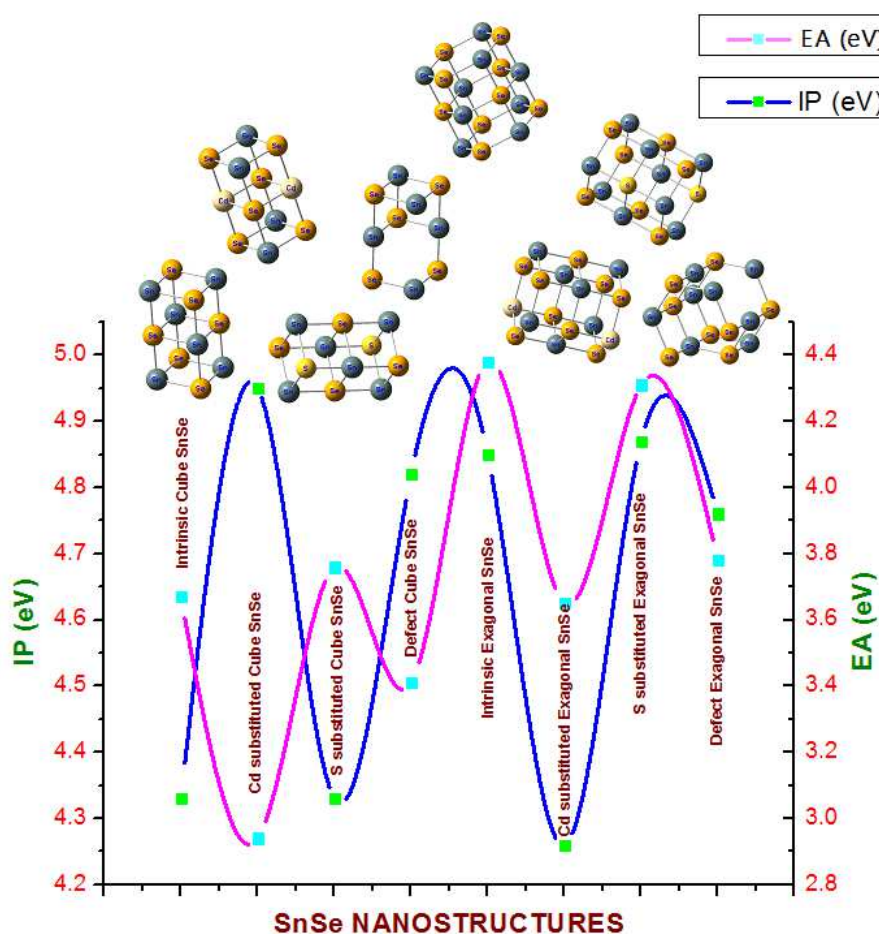
0.56



### 3.2. Ionization potential, Electron affinity, chemical potential and chemical hardness of SnSe nanostructures

Electron affinity (EA) and Ionization potential (IP) are used to describe the electronic properties of SnSe nanostructures [23]. Figure 2 denotes the graphical representation of EA and IP of SnSe nanostructures. IP is the energy required to remove electron from SnSe nanostructures and EA refers the change in the energy due to addition of electron in SnSe nanostructures. There is not much variation observed in IP and the values are in the range from 4.26 – 4.95 eV. However, the hexagonal SnSe nanostructure has low IP value rather than pure form of SnSe nanostructure. In contrast, substitution of Cd and S on hexagonal SnSe nanostructures results in low value of IP. Electron affinity plays a vital role in chemical sensors and Plasma Physics. Different trends are observed in EA of SnSe nanostructures. Cd substituted SnSe nanostructures has low value of EA, 2.94 eV for cube and 3.65 eV for hexagonal structure. Hence less energy is released due to addition of electron in Cd substituted SnSe nanostructures. The remaining SnSe nanostructures release more energy with the addition of electron.

Figure 2. IP and EA of SnSe nanostructures



CH and CP is also a key factor to define structural stability of SnSe nanostructures [24]. The CH and CP can be calculated as  $\eta = (IP - EA)/2$  and  $\mu = -(IP + EA)/2$  respectively. Almost same trends are observed for CP in the range from -3.95 to 4.6 eV. Chemical potential is nothing but a partial molar free energy. It is a form of potential energy that is released or absorbed during the chemical reaction. It also referred as electronegativity. The chemical hardness is the negative value of electronegativity. The CH of SnSe nanostructures is relatively low in the range of 0.23 to 1.0 eV.

Table 3. Chemical potential and chemical hardness of SnSe nanostructures

Nanostructures	Chemical potential $\mu$ (eV)	Chemical hardness $\eta$ (eV)
Pure cube SnSe	-4	0.33
Pure hexagonal SnSe	-4.61	0.23
defect cube SnSe	-4.11	0.7
defect hexagonal SnSe	-4.27	0.49
Cd substituted cube SnSe	-3.94	1
Cd substituted hexagonal SnSe	-3.95	0.3
S substituted cube SnSe	-4.04	0.28
S substituted hexagonal SnSe	-4.59	0.28

### 3.3. Vibrational analysis of CaSe nanostructures

Vibrational studies are used to deliberate the stability of SnSe nanostructures. All the possible SnSe nanostructures are more stable since there is no imaginary frequency observed as represented in Table 4 [25, 26].



Table 4: Vibrational Frequency and IR intensity of SnSe nanostructures

Nanostructures	Frequency (cm <sup>-1</sup> )		IR intensity (km/mole)	
Pure cube SnSe	469.53	411.03	55.42	37
Pure hexagonal SnSe	469.53	471.49	37.38	35.9
defect cube SnSe	419.61	249.84	32.38	30.83
defect hexagonal SnSe	273.08	487.62	27.61	11.46
Cd substituted cube SnSe	483.17	543.71	101.37	45.62
Cd substituted hexagonal SnSe	468.44	476.15	51.86	25.11
S substituted cube SnSe	486.97	500.04	64.01	48.08
S substituted hexagonal SnSe	475.99	501.01	43.62	37.18

Figure 3 (a). Pure cube SnSe nanostructure

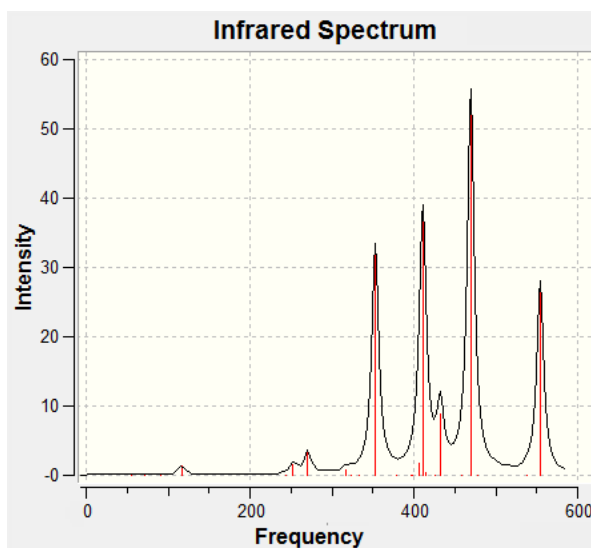


Figure 3 (b). Pure Hexagonal SnSe nanostructure

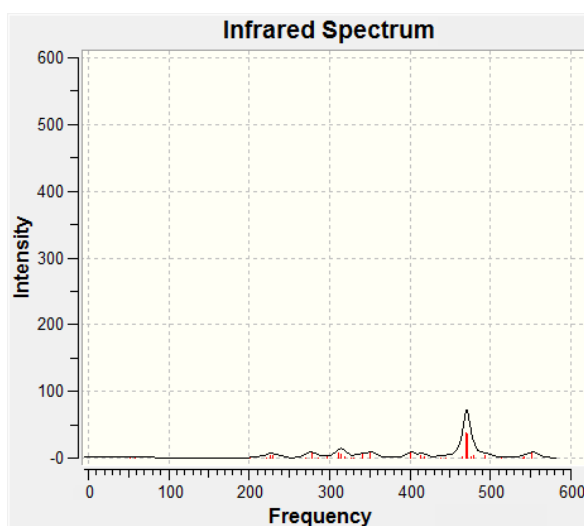


Figure 3 (c). defect cube SnSe nanostructure

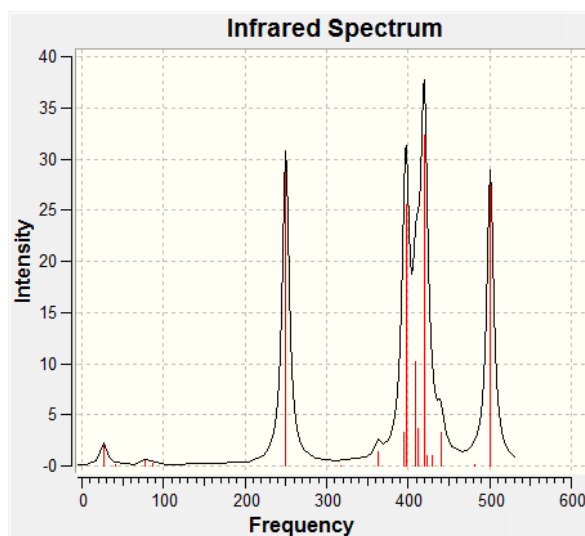


Figure 3 (d). defect hexagonal SnSe nanostructure

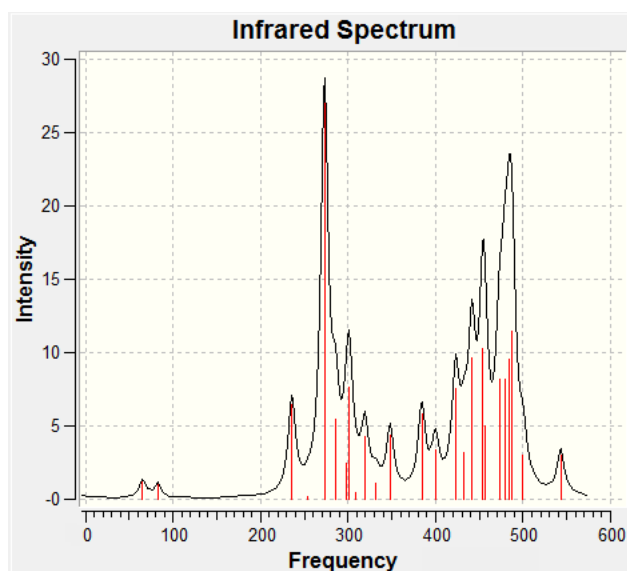


Figure 3 (e). Cd substituted cube SnSe nanostructure

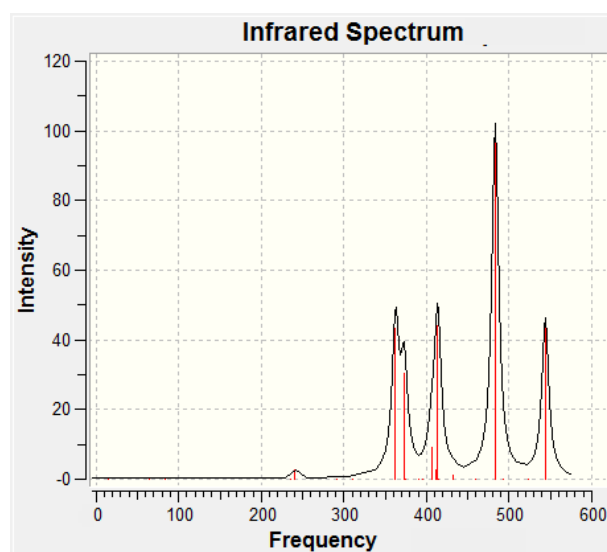


Figure 3 (f). Cd substituted hexagonal SnSe nanostructure

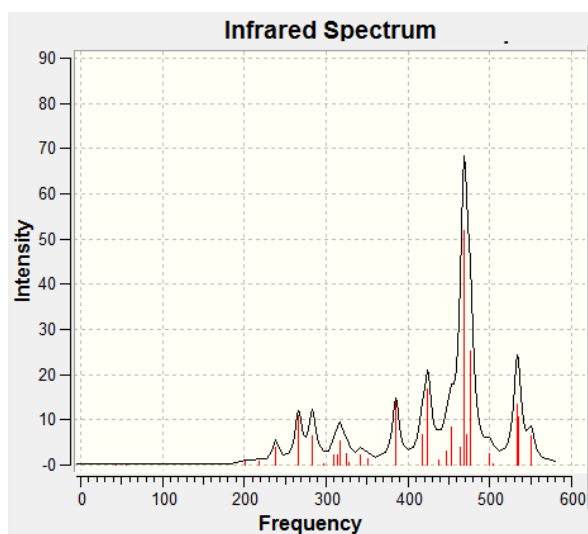


Figure 3 (g). S substituted cube SnSe nanostructure

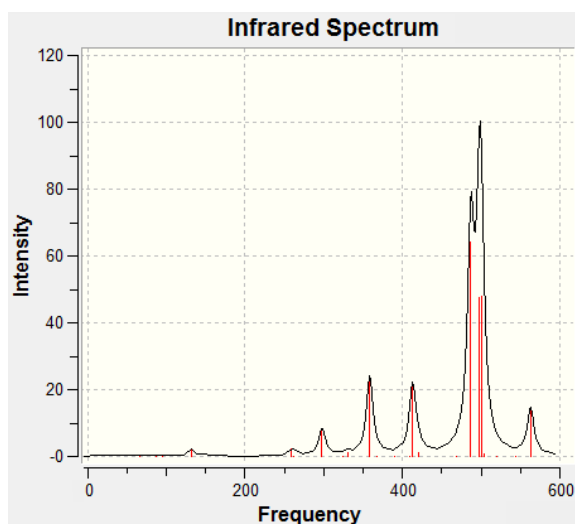
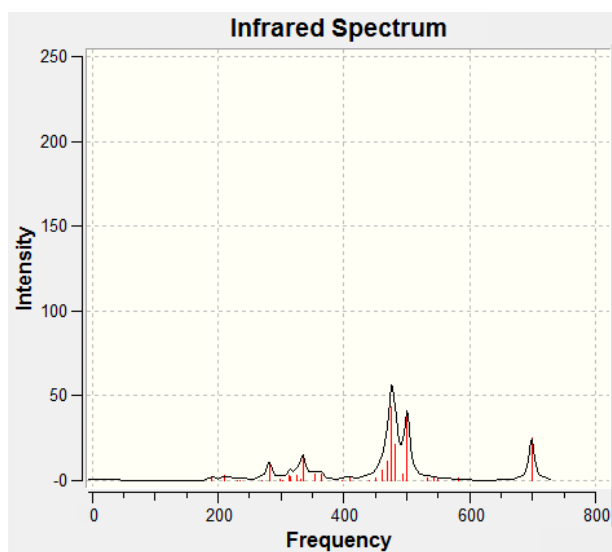


Figure 3 (h). S substituted hexagonal SnSe nanostructure



The pure cube SnSe nanostructure has the vibrational frequency at 469.53 and 411.03  $\text{cm}^{-1}$  with corresponding IR intensity of 55.42 and 37  $\text{km/mole}$ . Pure hexagonal SnSe nanostructures have prominent vibrational frequency at 469.53 and 471.49  $\text{cm}^{-1}$  with IR intensity of 37.38 and 35.9  $\text{km/mole}$  respectively. The prominent IR intensity of Cd substituted cube SnSe nanostructure is 101.37 and 45.62  $\text{km/mole}$  along with vibrational frequency at 483.17 and 543.71  $\text{cm}^{-1}$  respectively. Similarly, Cd substituted hexagonal SnSe nanostructure has the vibrational frequency at 468.44 and 476.15  $\text{cm}^{-1}$  and corresponds to IR intensity of 51.86 and 25.11  $\text{km/mole}$ . The S substituted cube SnSe nanostructure has vibrational frequency at 486.97 and 500.04  $\text{cm}^{-1}$  with IR intensity of 64.01 and 48.08  $\text{km/mole}$  respectively. The IR intensity of S substituted hexagonal SnSe nanostructure is 43.62 and 37.18  $\text{km/mole}$  with related vibrational frequency at 475.99 and 501.01  $\text{cm}^{-1}$ . Defect cube SnSe nanostructure has vibrational frequency at 419.61 and 249.84  $\text{cm}^{-1}$  along with prominent IR intensity of 32.38 and 30.83  $\text{km/mole}$ . Finally the vibrational frequency of defect hexagonal SnSe nanostructure is 273.08 and 487.62  $\text{cm}^{-1}$  and associated IR intensity recorded at 27.61 and 11.46  $\text{km/mole}$ . In all possible SnSe nanostructure, molecular stretching vibrational mode is observed. The vibrational spectrum of SnSe nanostructures are illustrated in Figure 3(a) – 3(h).

## CONCLUSION

DFT is utilized to study pure, defect structure, cadmium and sulfur substituted cube & hexagonal SnSe nanostructures and are successfully simulated using B3LYP/ LanL2DZ basis set. The structural stability of SnSe nanostructures are characterized by calculated energy and vibrational studies. Point symmetry, dipole moment, chemical potential and chemical hardness of all possible nanostructures of SnSe are reported. Electronic properties of SnSe nanostructures are discussed in terms of ionization potential, HOMO – LUMO gap, density of states and electron affinity. In the present work, the structural stability and electronic properties can be fine-tuned with substitution impurities and defect in the structure. The electronic properties and structural stability of SnSe nanostructures can be improved which finds its potential importance in optoelectronic applications.

## REFERENCES

- [1] R. Waser, *Nanoelectronics and Information Technology; Materials, Processes, Devices*, Wiley, New York, **2002**.
- [2] C. R. Baxter, W. D. McLennan, *J. Vac. Sci. Technol.*, **1975**, 12, 110.
- [3] N. R. Mathews, *Solar Energy*, **2011**, 86, 1010.
- [4] K. M. Chung, D. Wamwangi, M. Woda, M. Wuttig, W. Bensch, *J. Appl. Phys.*, **2008**, 103, 083523.
- [5] D. P. Padiyan, A. Marikani, K. R. Murali, *Cryst. Res. Technol.*, **2000**, 35(8), 949.
- [6] N. Kumar, V. Sharma, U. Parihar, R. Sachdeva, N. Padha, C. J. Panchal, *J. Nano- Electron. Phys.*, **2011**, 3(1), 117.
- [7] Z. Zainal, N. Saravanan, K. Anuar, M. Z. Hussein, W. M. M. Yunus, *Mater. Sci. Eng. B*, **2004**, 107(2), 181.
- [8] G. H. Chandra, J. Naveen Kumara, N. M. Raob, S. Uthanna, *J. Cryst. Growth*, **2007**, 306, 68.
- [9] V. E. Drozd, I. O. Nikiforova, V. B. Bogevolnov, A. M. Yafyasov, E. O. Filatova, D. Papazoglou, *J. Phys. D.*, **2009**, 42, 125306.
- [10] J. P. Singh, R. K. Bedi, *J. Appl. Phys.*, **1990**, 68, 2776.
- [11] R. Chandiramouli, S. Sriram, D. Balamurugan, *Mol. Phys.*, **2014**, 112, 151.
- [12] V. Nagarajan R. Chandiramouli, *Res J Pharm Biol Chem Sci.*, **2014**, 5(1), 365.
- [13] V. Nagarajan, R. Chandiramouli, *Int. J. ChemTech Res.*, **2014**, 6(1), 21.
- [14] M. Valiev, E. J. Bylaska, N. Govind, K. Kowalski, T.P. Straatsma, H.J.J. Van Dam, D. Wang, J. Nieplocha, E. Apra, T.L. Windus, W. A. De Jong, *Comput Phys Commun.*, **2010**, 181, 1477.
- [15] R. Chandiramouli, *Res. J. Chem. Environ.*, **2013**, 17, 64.
- [16] A. Droghetti, D. Alfè, S. Sanvito, *J. Chem. Phys.*, **2012**, 137, 124303.
- [17] Mohammed Bouklah, Houria Harek, Rachid Touzani, Belkheir Hammouti, Yahia Harek, *Arabian J. Chem.*, **2012**, 5, 163.
- [18] Wei Huang, *J. Chem. Phys.*, **2009**, 131, 234.
- [19] G.S. Groenewold, A. K. Gianotto, M.E. McIlwain, J. Van Stipdonk Michael, Kullman Michael, T. Moore David, Polfer Nick, Oomens Jos, Infante Ivan, Visscher Lucas, Siboulet Bertrand and A.de Jong Wibe, *J. Phys. Chem.*, **2008**, 112 A, 508.
- [20] R. Srinivasaraghavan, R. Chandiramouli, B.G. Jeyaprakash, S. Seshadri, *Spectrochim. Acta, Part A.*, **2013**, 102, 242.
- [21] R. John Xavier, E. Gobinath, *Spectrochim. Acta, Part A.*, **2012**, 97, 215.
- [22] S. Sriram, R. Chandiramouli, D. Balamurugan, A. Thayumanvan, *Eur. Phys. J. Appl. Phys.*, **2013**, 62, 30101.
- [23] C.G. Zhan, J.A. Nichols, D.A. Dixon, *J. Phys. Chem.*, **2003**, 107 A, 4184.
- [24] R.G. Pearson, *J. Am. Chem. Soc.*, **1986**, 108, 6109.
- [25] D. Bandyopadhyay, *J. Mol. Model.* **2012**, 18,737.

[26] V. Nagarajan , R. Chandiramouli, *Der Pharma Chemica*, 2014, 6, 37.